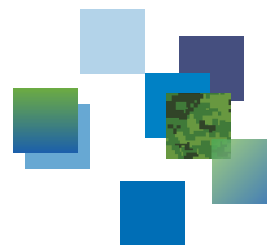




Defence Research and  
Development Canada

Recherche et développement  
pour la défense Canada

DRDC | RDDC



## DRDC Starfish Acoustic Sentinel and Phase Gradient Histogram Tracking

C.E. Lucas

G.J. Heard

N. Pelavas

DRDC – Atlantic Research Centre

**Defence Research and Development Canada**

Scientific Report

**DRDC-RDDC-2015-R025**

April 2015



# **DRDC Starfish Acoustic Sentinel and Phase Gradient Histogram Tracking**

C.E. Lucas

G.J. Heard

N. Pelavas

DRDC – Atlantic Research Centre

**Defence Research and Development Canada**

Scientific Report

DRDC-RDDC-2015-R025

April 2015

© Her Majesty the Queen in Right of Canada (Department of National Defence), 2015

© Sa Majesté la Reine en droit du Canada (Ministère de la Défense nationale), 2015

# Abstract

---

DRDC - Atlantic Research Centre, an agency of the Canadian Department of National Defence, has developed a prototype multi-influence underwater surveillance sensor called the Starfish. The Starfish has acoustic, electric, and magnetic field sensors, and onboard signal processing for target detection and tracking. The acoustic sensors are in the form of a seven-element cross-dipole hydrophone array, with two hydrophones along each orthogonal axis direction and one at the array centre.

Acoustic target detection is performed using both time-domain and frequency-domain Sentinel algorithms. The Sentinel algorithms use parallel exponential filters, with the frequency-domain algorithm using parallel filters in each frequency bin.

A Phase Gradient bearing estimation algorithm is used to perform the acoustic target tracking. This is a frequency-domain algorithm that estimates the gradient of the spatial phase of the incoming acoustic signal, and directly computes the wavevector of the acoustic arrival in each frequency bin. A Histogram Tracking procedure is used to display and determine the track angles for a broad-band acoustic target. This paper will discuss the details of the frequency-domain Acoustic Sentinel algorithm and the Phase Gradient bearing estimation algorithm with Histogram Tracking.

## Significance for defence and security

---

For the Force ASW project, the DRDC Starfish sensor units provide underwater sensor capability for acoustic target detection and tracking. The DRDC Starfish units use a seven-element three-dimensional acoustic hydrophone array to sample the local underwater acoustic environment, and have onboard signal processing to determine the presence and track of a broad-band acoustic target. The Starfish autonomous sensor systems with their detection and tracking algorithms give the Canadian Forces surveillance capability to detect surface and subsurface acoustic targets in littoral waters and choke points.

# Résumé

---

Le Centre de recherches de l'Atlantique de RDDC, une agence du ministère de la Défense nationale, a mis au point un prototype de capteur de surveillance sous-marine à influences multiples appelé Starfish. Le Starfish est muni de capteurs acoustiques, électriques et de profondeur de champ magnétique en plus d'une unité embarquée de traitement du signal pour la détection et la poursuite de cibles. Les capteurs acoustiques sont constitués d'un réseau hydrophonique de dipôles croisés à sept composantes, soit deux hydrophones dans chaque axe orthogonal et un autre au centre du réseau.

Les cibles acoustiques sont détectées au moyen des algorithmes Sentinel dans le domaine temporel et le domaine fréquentiel. Ces algorithmes font appel à des filtres exponentiels parallèles ; dans le domaine fréquentiel, l'algorithme utilise des filtres parallèles dans chaque cellule de fréquences.

Un algorithme d'estimation d'azimut du gradient de phase sert à la poursuite des cibles acoustiques. Il s'agit d'un algorithme dans le domaine fréquentiel qui permet d'évaluer le gradient de la phase spatiale du signal acoustique entrant et de calculer directement le vecteur d'onde d'arrivée dans chaque cellule de fréquences. Une procédure de poursuite par histogramme sert à déterminer et à afficher les angles de route des cibles acoustiques à large bande. Le présent article expose en détail l'algorithme acoustique Sentinel dans le domaine fréquentiel et l'algorithme d'évaluation d'azimut du gradient de phase avec poursuite par histogramme.

## Importance pour la défense et la sécurité

---

Pour le projet de guerre anti-sous-marine (GASM) de la force, le Starfish de RDDC fournit une capacité sous-marine de détection et de poursuite de cibles acoustiques. Les capteurs Starfish de RDDC utilisent un réseau hydrophonique tridimensionnel à sept composantes pour échantillonner l'environnement acoustique sous-marin, et ils sont dotés d'une unité embarquée de traitement du signal pour déterminer la présence d'une cible acoustique à large bande et la poursuivre. Les systèmes autonomes de détection Starfish et leurs algorithmes de détection et de poursuite procurent aux Forces armées canadiennes une capacité de surveillance permettant de détecter les cibles acoustiques à la surface et sous la surface des eaux littorales et des points de passage obligé.

# Table of contents

---

Abstract . . . . .	i
Significance for defence and security . . . . .	i
Résumé . . . . .	ii
Importance pour la défense et la sécurité . . . . .	ii
Table of contents . . . . .	iii
List of figures . . . . .	iv
1 Introduction . . . . .	1
2 Frequency-domain acoustic sentinel . . . . .	1
3 Phase Gradient bearing estimation algorithm . . . . .	4
3.1 Phase Gradient development . . . . .	6
3.2 Orthogonal array Phase Gradient . . . . .	7
3.3 Tetra array Phase Gradient . . . . .	8
4 Comparison of Phase Gradient to other DOA algorithms . . . . .	9
4.1 Average Histogram method . . . . .	9
4.2 Average Direction Cosine method . . . . .	11
4.3 Simulation results . . . . .	11
5 Phase Gradient Histogram Tracking example . . . . .	12
6 Conclusion . . . . .	14
References . . . . .	17

# List of figures

---

Figure 1:	Second generation of the DRDC Starfish sensor node. . . . .	2
Figure 2:	Normalized frequency response of the two exponential digital filters used in the Starfish Acoustic Sentinel algorithm. . . . .	4
Figure 3:	Responses and resulting fast to slow ratio of the two exponential digital filter outputs to a target pass, for one FFT bin. The input to the filters is the average spectral power for that FFT bin at each time window. . . . .	5
Figure 4:	The hydrophone array (of diameter $d$ ) for which the Phase Gradient algorithm was designed. . . . .	6
Figure 5:	The Tetra hydrophone array for which the Phase Gradient algorithm was adapted. . . . .	8
Figure 6:	Phase Gradient bearing histogram, un-smoothed (top) and smoothed (bottom) for one simulation at 12 dB SNR and DOA of $45^\circ$ . A Gaussian shape is fitted to the histograms. . . . .	10
Figure 7:	Estimates of the DOA from all algorithms for 100 simulations, with SNR $-3$ dB and the true DOA at $45^\circ$ . . . . .	11
Figure 8:	Mean and Standard Deviations of the estimated DOA for 100 simulations, as a function of Signal to Noise Ratio (SNR). The true DOA is at $45^\circ$ , indicated by the dashed line. . . . .	12
Figure 9:	Horizontal bearings from the Phase Gradient algorithm, with color coded bearing as a function of time and frequency. . . . .	13
Figure 10:	Histogram tracking of the horizontal bearing using the Phase Gradient algorithm, with color coded histogram counts. . . . .	14



# 1 Introduction

---

The DRDC - Atlantic Research Centre has had a multi-year research and development program to create a prototype underwater multi-influence sensor package for littoral surveillance applications. The prototype sensors, shown in Fig. 1, are in their second generation and are called Starfish sensor nodes. The Starfish nodes are designed to be deployed in up to 500 m water depth. Each Starfish sensor node contains a low-noise, high sensitivity tri-axial magnetometer, three Underwater Electric Potential sensors, a seven-element crossed-dipole hydrophone array, a wide-band hydrophone, and a combined 3D gravitational and magnetic orientation sensor. Each Starfish node contains a powerful onboard ARM processor that runs an embedded version of the Linux operating system. The processor is powerful enough to perform real-time acquisition, storage, and signal processing of the sensor data. Target detection and tracking results from the onboard processing are relayed through an attached cable or a network of underwater acoustic modems to a surface gateway buoy, which has a wireless radio frequency link to shore. Each Starfish node contains internal solid-state memory storage where sensor data may also be logged for later analysis. The Starfish nodes may be deployed with or without cables to shore. When deployed without cables, each Starfish node can run autonomously for more than five days of continuous use, or for several weeks in a wake-on-detection mode. This paper describes the acoustic processing running onboard the Starfish sensor node. The acoustic processing proceeds as follows: first the acoustic Sentinel algorithm determines if there is an acoustic target nearby, second the acoustic tracking algorithm using the Phase Gradient bearing estimation algorithm with Histogram Tracking determines the target's bearing and bearing change rate, and finally a compact NILUS protocol message [1] is generated and transmitted to the user over the communications network.

## 2 Frequency-domain acoustic sentinel

---

The Starfish Cubes have two algorithms that determine if an acoustic target is present, the time-domain and the frequency-domain Acoustic Sentinel. The time-domain Acoustic Sentinel calculates the average power from the array centre hydrophone, and passes this value into two exponential filters, one with a long time constant and one with a shorter time constant. The ratio of the outputs of the fast to slow filters is used to determine if a target is present. Similarly, the frequency-domain Acoustic Sentinel algorithm works on Fast Fourier Transform (FFT) processed data collected from the centre hydrophone of the crossed-dipole hydrophone array. Each channel of the hydrophone array is sampled at a rate of 2500 samples per second, and is low-pass filtered with a 700 Hz cutoff frequency. The typical frequency band for frequency-domain Acoustic Sentinel processing is 50 Hz to 500 Hz. The frequency-domain Sentinel algorithm uses a bank of exponential digital filters, two filters for



**Figure 1:** Second generation of the DRDC Starfish sensor node.

each FFT frequency bin in the processing bandwidth. The input to each pair of filters is the average power spectrum value obtained from the FFT processing for that frequency bin. The general input-output relationship of the exponential filter is given by Eqn. (1),

$$\begin{aligned} y(n) &= (1 - \alpha)x(n) + \alpha y(n - 1), & n \geq 0 \\ &= (1 - \alpha) \sum_{k=0}^n \alpha^k x(n - k) \end{aligned} \quad (1)$$

and where  $x(n) = y(n) = 0$  for  $n < 0$ . In Eqn. (1),  $x(n)$  and  $y(n)$  are the filter input and output respectively at sample  $n$ . The parameter  $\alpha$  determines the low-pass cut-off frequency of the filter,  $0 < \alpha < 1$ . With each frequency bin we associate two filters with different  $\alpha$  values. As seen from the second line of Eqn. (1), the slow filter, with larger  $\alpha$  value, averages over more previous inputs  $x(n)$  than the fast filter with the smaller  $\alpha$  value. The slow filter output is referred to as the long-term average, and the fast filter output as the short-term average. The slow filter output will track input signals such as background noise that changes slowly over time, and reject shorter period signals. The fast filter output will respond more quickly to a shorter period target signal. Comparing the two filter outputs in a ratio of the fast to slow will give a measure that can be used to detect a target passage, while adjusting to gradual changes in the background ambient noise.

Both the time-domain and frequency-domain Acoustic Sentinel algorithms are available for acoustic target detection on the Starfish sensor nodes. This allows us to experimentally compare the detection performance of the algorithms to different acoustic

targets and in different environmental conditions. The Starfish sensor nodes were designed to detect acoustic targets in water depths up to 500 m. The frequency band for detection in the Starfish sensor node is 50 Hz to 500 Hz. In this band the typical surface and sub-surface targets that the Starfish sensor nodes were designed to detect have characteristically broad-band acoustic signatures. The frequency-domain Acoustic Sentinel was designed to take advantage of the broad-band nature of the expected target signatures, and reject any narrow-band acoustic energy in the environment that may be present. A possible disadvantage of the frequency-domain algorithm is that a strong target with a narrow-band acoustic spectrum could be missed, whereas the time-domain algorithm essentially integrates the energy in the whole band. Since both the frequency-domain and time-domain Sentinel algorithms can be running simultaneously, the detection differences between the algorithms could be used for possible target type discrimination, or to flag an unusual or unexpected acoustic environment. The frequency-domain algorithm allows for better optimization of detection performance because there are more algorithm parameters that can be tuned for particular target and signature type.

In the frequency-domain Acoustic Sentinel algorithm we often use 1024-point FFTs with 50% overlap to compute the average spectrum. Typically, a total of 6 FFTs are used for the averaging, with the last 2 FFTs being used in the next group of 6 FFTs. This results in an average spectral power value input to the parallel filters, in each frequency bin, once every 2048 samples, or at an effective sample rate of  $f_s = 1.22$  Hz. For the slow and fast response filters, the parameter  $\alpha$  has the default values of 0.999 and 0.9, respectively. The frequency response of the filters with these two  $\alpha$  values is shown in Fig. 2. The rise-time of the slow filter is  $\approx 30$  minutes, and for the fast filter  $\approx 20$  seconds, when data is sent to the filters at a rate of  $f_s = 1.22$  Hz.

The frequency-domain Acoustic Sentinel algorithm will trigger acoustic target detection when a programmable specified percentage (*e.g.*, 60%) of the frequency bins in the 50 Hz to 500 Hz band exceed a programmable ratio threshold value (*e.g.*, 3). We expect the frequency-domain algorithm to detect a target if the broad-band signal to noise ratio (SNR)  $\approx 6$  dB or greater. A target lost message is triggered when another percentage (*e.g.*, 80%) of the bins fall below another ratio threshold parameter value (*e.g.*, 2). Using percentages of the bins as target detect and lost threshold parameters means that not all of the same bins have to hold the required ratio threshold level. Some bins at a certain time step may fall below the ratio threshold value when going to the next time step, but other bins may increase over the ratio threshold, so that the percentage of bins above the target detect threshold is the same.

The FFT lengths and overlap values, the percentage of the bins above and below the threshold values, the threshold levels, and the frequency band range, are all algorithm parameters that are programmable in the Starfish sensor node. Fig. 3 shows an example of the filter responses and resulting ratio of the fast to slow filter

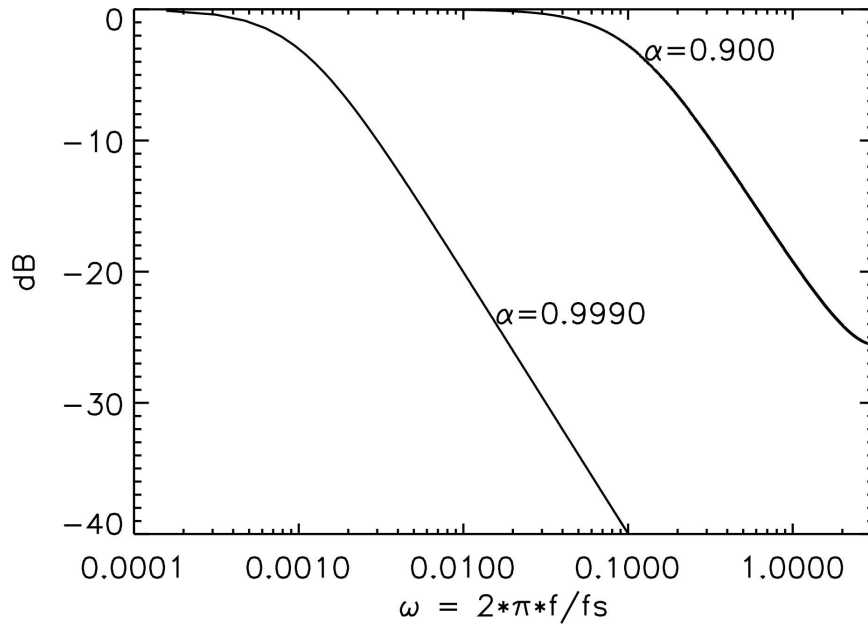


**Figure 2:** Normalized frequency response of the two exponential digital filters used in the Starfish Acoustic Sentinel algorithm.

outputs for a real target pass, for one FFT bin at 300 Hz. This was a particularly slow target pass of a distant target, and the filter slow and fast  $\alpha$  parameters were adjusted to 0.999 and 0.99 respectively for this target.

### 3 Phase Gradient bearing estimation algorithm

---

The Phase Gradient algorithm was originally designed as part of a homing system for an Autonomous Underwater Vehicle (AUV) [2]. In the flooded nose cone section of the AUV a tri-axis cross-dipole, seven-element hydrophone array was mounted and used to estimate the bearing and elevation angles to a single frequency beacon signal. A frequency-domain bearing estimation algorithm was the natural choice to determine the Direction of Arrival (DOA), to take advantage of the increase in SNR in going to the frequency-domain when processing a tonal signal. The on-board processing capability of the AUV was unfortunately not sufficient to implement the Conventional (Bartlett) and Minimum Variance Distortionless Response (MVDR) DOA algorithms. This motivated the development of the Phase Gradient Algorithm for the single frequency case.

Both the Conventional and MVDR beamforming algorithms require forming beams and calculating a beampower for a large set of discreet look directions, typically

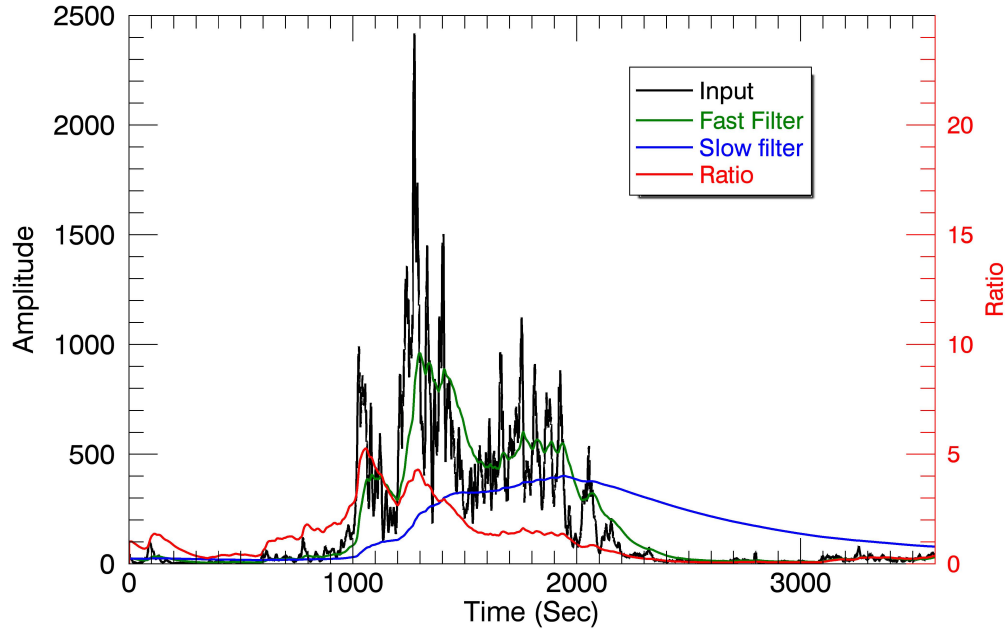


**Figure 3:** Responses and resulting fast to slow ratio of the two exponential digital filter outputs to a target pass, for one FFT bin. The input to the filters is the average spectral power for that FFT bin at each time window.

searching over  $360^\circ$  in horizontal bearing and from  $-90^\circ$  to  $90^\circ$  in elevation angle. After calculating beampowers over all combinations of bearing and elevation angles, the single look direction that gives the maximum output beampower with its associated bearing and elevation angle define the DOA of the incoming plane wave. This searching over bearing and elevation used by the Conventional and MVDR algorithms requires significant processing power. In contrast, the Phase Gradient algorithm directly estimates the three Cartesian components of the incoming signal wavevector from estimated cross-spectra between the hydrophone elements. It is robust against hydrophone failure, and every hydrophone in the array is used to estimate each component of the wavevector. The Phase Gradient algorithm does not require searching over bearing and elevation angles and calculating a beampower at each look direction, so it is very computationally efficient. The Phase Gradient algorithm was able to calculate the bearing and elevation angles to the homing beacon signal at the update rate required by the AUV homing system. This algorithm is well suited for bearing estimation in embedded systems that have limited processing power.

### 3.1 Phase Gradient development

We consider a planar acoustic wave incoming to a hydrophone array from a fixed direction of arrival, as shown in Fig. 4. We define  $s(t)$  as the time domain signal present at hydrophone #0 due to the plane wave arrival, in the absence of any noise. We define the vector  $\hat{k}_s$  as the unit vector that points in the direction of travel of the incoming wave. We define  $x_i(t)$ ,  $i = 0 \dots 6$  as the time domain signals measured by the hydrophones, including noise. The time domain signal  $x_i(t)$  measured at the  $i^{th}$  hydrophone, in terms of  $s(t)$  is given by

$$x_i(t) = s \left( t - \frac{\hat{k}_s \circ \vec{r}_i}{c} \right) + n_i(t) . \quad (2)$$

Here we have defined  $\vec{r}_i$  as the position vector to the  $i^{th}$  hydrophone, and  $c$  as the speed of sound in water. The term  $n_i(t)$  represents the noise present on the  $i^{th}$  hydrophone that is uncorrelated to the incoming signal. The measured hydrophone time series  $x_i(t)$  are delayed or advanced versions of  $s(t)$  with noise added, the delay times depending on the direction of arrival of the incoming signal.

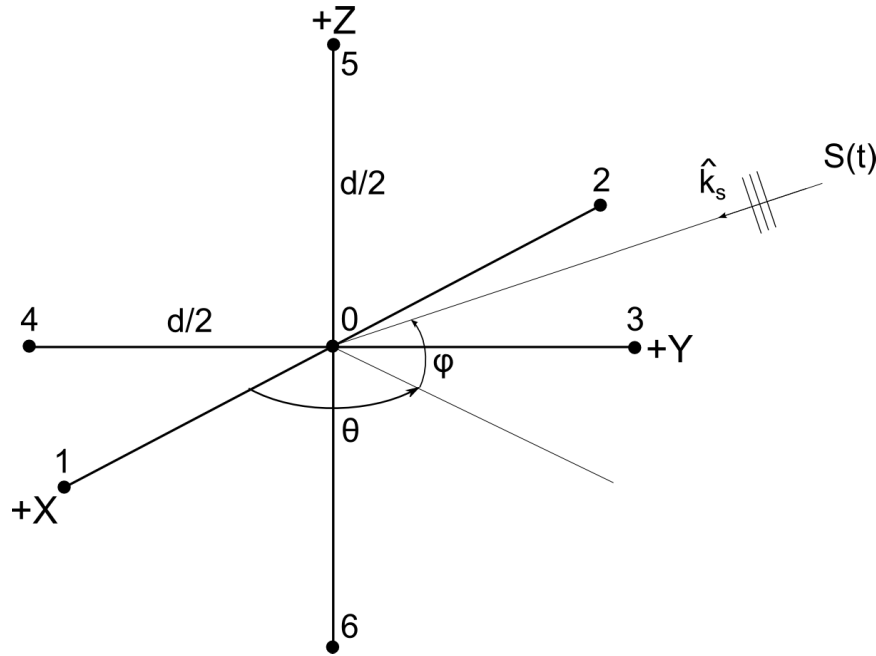


**Figure 4:** The hydrophone array (of diameter  $d$ ) for which the Phase Gradient algorithm was designed.

If we take the Fourier Transform of Eqn. (2), we obtain the frequency domain representation of the hydrophone outputs, given by

$$\begin{aligned} X_i(f) &= S(f) \exp \left( -j \vec{k}_s \circ \vec{r}_i \right) + N_i(f) \\ &= |S(f)| \exp \left( -j \vec{k}_s \circ \vec{r}_i + j \angle S(f) \right) + N_i(f) . \end{aligned} \quad (3)$$

The frequency domain representation of the time signals is denoted by capital letters, and  $j$  is the imaginary unit. The Argument of  $S(f)$  is denoted by  $\angle S(f)$ . The incoming signal wavevector  $\vec{k}_s = |\vec{k}_s| \hat{k}_s = \frac{2\pi f}{c} \hat{k}_s$  of Eqn. (3) is a function of frequency. From Eqn. (3) we can see that for a given frequency, the spatial phase at any position vector  $\vec{r}$  of the incoming signal, neglecting noise, is given by

$$\psi(\vec{r}) = -\vec{k}_s \circ \vec{r} + \angle S(f) . \quad (4)$$

The phase angle  $\angle S(f)$  does not depend upon the spatial position vector  $\vec{r}$ , and will have zero gradient. If we can estimate the gradient of the spatial phase  $\psi(\vec{r})$  we will have an estimate of the wavevector  $\nabla \psi(\vec{r}) = -\vec{k}_s$ , and thus have the arrival direction.

### 3.2 Orthogonal array Phase Gradient

We estimate the gradient of the spatial phase given by Eqn. (4), for the cross-dipole array of Fig. 4, from the Argument of a modified definition of the cross-spectrum between two hydrophones. We define  $X_i$  as being the complex FFT spectral value in a particular frequency bin for the  $i^{th}$  hydrophone. Here we write  $\vec{k}_s$  in Cartesian coordinates  $\vec{k}_s = (k_x, k_y, k_z)$ , use  $\langle \rangle$  to denote expectation value, and  $\psi_i$  to denote the phase of the  $i^{th}$  hydrophone. With the array diameter being denoted by  $d$ , we have for the  $x$ -axis direction a "new" cross-spectrum defined as

$$\begin{aligned} \langle X_1 X_2^* \rangle_{new} &= \langle X_1 (X_0 + X_3 + X_4 + X_5 + X_6)^* + (X_0 + X_3 + X_4 + X_5 + X_6) X_2^* \rangle \\ &= 2 \langle SS^* \rangle \left( 1 + 2 \cos(k_y \frac{d}{2}) + 2 \cos(k_z \frac{d}{2}) \right) e^{j \frac{1}{2}(\psi_1 - \psi_2)} . \end{aligned} \quad (5)$$

In Eqn. (5) the phase contributions from the  $y$  and  $z$ -axis directions combine to create a real-valued amplitude factor depending on  $k_y$  and  $k_z$  because of the array symmetry, leaving only half the phase difference between hydrophones #1 and #2 as the Argument of the complex exponential. Using the "new" cross-spectrum ensures that all the array hydrophones are used in the estimate of the phase difference. We can estimate the  $x$ -component of  $\nabla \psi(\vec{r})$  from

$$\frac{2 \angle \langle X_1 X_2^* \rangle_{new}}{d} = \frac{\psi_1 - \psi_2}{d} = \frac{\partial \psi}{\partial x} . \quad (6)$$

For the  $y$  and  $z$ -axis directions we can perform similar operations to Eqs. (5) and (6), obtaining the remaining components of  $\nabla \psi(\vec{r}) = -\vec{k}_s$  and the direction of arrival. We estimate the bearing and elevation angles from the wavevector components in each frequency bin from

$$\theta = \arctan \left( \frac{k_y}{k_x} \right) , \quad \phi = \arctan \left( \frac{k_z}{\sqrt{k_x^2 + k_y^2}} \right) . \quad (7)$$

### 3.3 Tetra array Phase Gradient

The Phase Gradient algorithm has been adapted for use with a 4-element tetrahedral array shape [3]. Fig. 5 shows the Tetra array geometry, where  $d = 0.162$  m is the distance from the origin to each  $x - y$  plane hydrophone, and  $d_z = 0.228$  m is the height of the top hydrophone above the  $x - y$  plane. We estimate the arrival angles from the components of the wavevector using Eq. (7). The wavevector components for the Tetra geometry are given by Eq. (8).

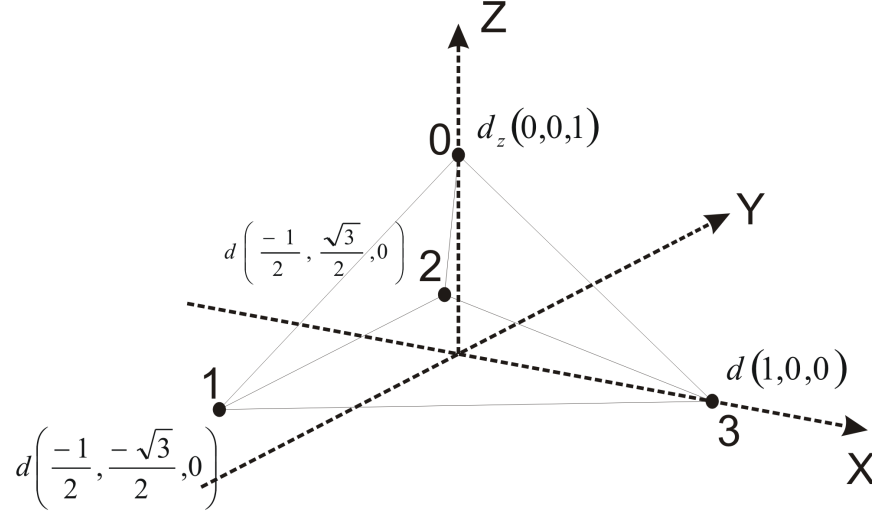


**Figure 5:** The Tetra hydrophone array for which the Phase Gradient algorithm was adapted.

$$\begin{aligned}
 k_x &= \frac{1}{d} \text{Arg} \left\{ \langle X_0 X_1^* \rangle^{\frac{1}{6}} \langle X_0 X_2^* \rangle^{\frac{1}{6}} \langle X_3 X_0^* \rangle^{\frac{1}{3}} \langle X_3 X_1^* \rangle^{\frac{1}{6}} \langle X_3 X_2^* \rangle^{\frac{1}{6}} \right\}, \\
 k_y &= \frac{2}{\sqrt{3}d} \text{Arg} \left\{ \langle X_0 X_1^* \rangle^{\frac{1}{6}} \langle X_2 X_0^* \rangle^{\frac{1}{6}} \langle X_2 X_1^* \rangle^{\frac{1}{6}} \langle X_3 X_1^* \rangle^{\frac{1}{6}} \langle X_2 X_3^* \rangle^{\frac{1}{6}} \right\}, \\
 k_z &= \frac{1}{d_z} \text{Arg} \left\{ \langle X_0 X_1^* \rangle^{\frac{1}{3}} \langle X_0 X_2^* \rangle^{\frac{1}{3}} \langle X_0 X_3^* \rangle^{\frac{1}{3}} \right\}.
 \end{aligned} \tag{8}$$



## 4 Comparison of Phase Gradient to other DOA algorithms

---

When considering DOA algorithms to implement on the second generation Starfish sensor nodes the Phase Gradient algorithm and MVDR algorithms were chosen. The Phase Gradient algorithm was chosen because of its good performance in the AUV homing system at a single frequency. This was a good opportunity to extend the use of the algorithm to broad-band signals, and to experimentally evaluate its performance on a 7-element cross-dipole array shape. The MVDR algorithm was chosen because of its performance in simulations, and its ability to resolve more than one DOA signal simultaneously. Both algorithms are similar in that they both are frequency-domain algorithms that result in a DOA bearing estimate in each FFT frequency bin. In computer simulations the performance of both of these algorithms was compared to the performance of the standard time-domain crossed-dipole DOA algorithm used in DIFAR sonobuoys. The DIFAR time-domain algorithm [4] will be referred to here as the DIFAR TD algorithm.

In the computer simulations the dipole array diameter was set to 0.4 m, the sound speed 1490 m/s, the sample rate 8000 samples per second. Time blocks of 10 second duration were used, and for the frequency-domain algorithms the FFT lengths were set to 8000 points. The required average spectra were calculated using 50% overlap for a total of 19 averages per time block. The plane wave arrival signal and the noise on each hydrophone were simulated as broad-band gaussian white noise sequences. A single 10 second time block with 80000 samples is considered as one simulation, which produces one bearing estimate (only horizontal bearings are considered in this paper) from each DOA algorithm. The true DOA bearing for the simulations was set to  $45^\circ$ . All the processing was performed in the frequency band of 50 Hz to 500 Hz.

### 4.1 Average Histogram method

For both the Phase Gradient and MVDR algorithms we get an estimate of the DOA of the incoming plane wave signal at each FFT frequency bin in the band of interest. Two approaches were used to estimate a single DOA value from the frequency domain information in all the bins.

The first approach was to calculate the bearing in each frequency bin and then create a histogram of the bearings. We divide the horizontal bearing range of  $-180^\circ$  to  $+180^\circ$  into a set of equally spaced bearing bins of  $1^\circ$  width. For one simulation we get a bearing estimate at each FFT frequency bin. For every frequency bin, we add one count to the bearing bin whose associated bearing range contains the DOA estimate. The sum of all the counts over all the bearing bins equals the number of FFT frequency

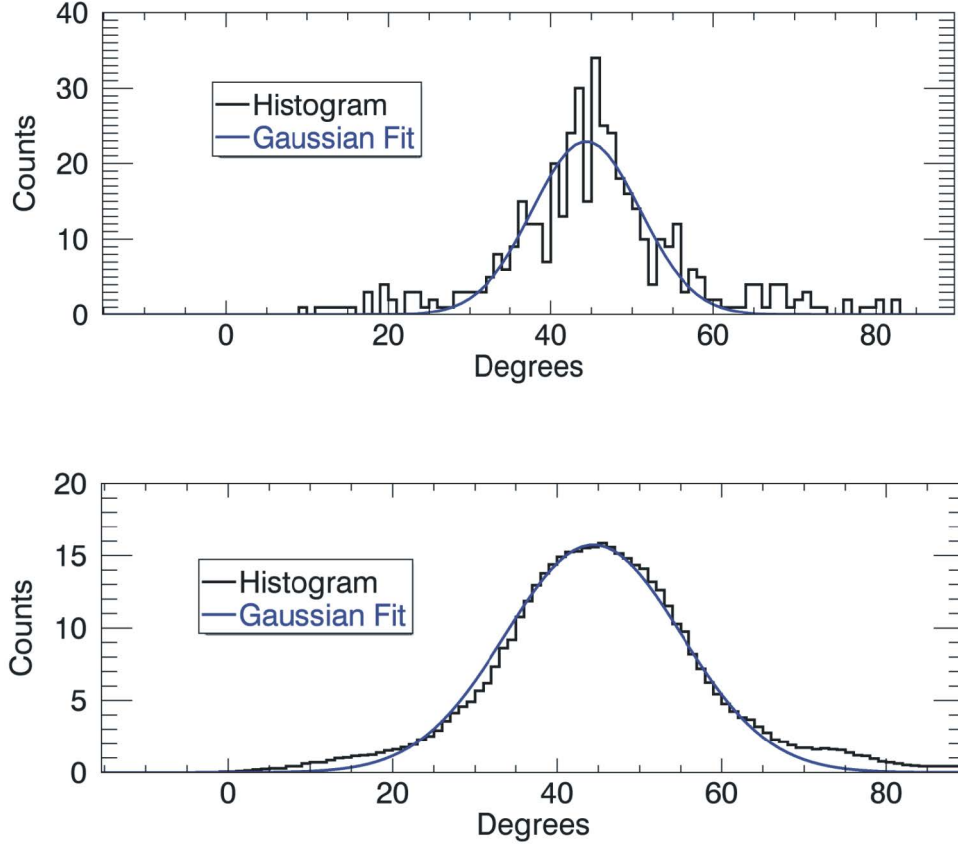


**Figure 6:** Phase Gradient bearing histogram, un-smoothed (top) and smoothed (bottom) for one simulation at 12 dB SNR and DOA of  $45^\circ$ . A Gaussian shape is fitted to the histograms.

bins. Fig. 6 shows a Phase Gradient bearing histogram, un-smoothed and smoothed for a single simulation, with the true DOA set at  $45^\circ$  and the SNR 12 dB. We can see that the smoothed histogram is approaching a Gaussian distribution shape. The arctangent DOA estimator is an unbiased estimator [5], and its probability density function (pdf) is estimated from the smoothed histogram. A 21-point boxcar average was used for smoothing, which creates real-valued histogram counts. To estimate the DOA we then perform a sum of the pdf times the bearing value over a  $31^\circ$  width about the peak. Summing over the peak prevents bearings that are too far away from the peak to be included in the DOA estimate. The same procedure is performed for the MVDR algorithm with similar results, although the Phase Gradient algorithm estimated pdf has a noticeably smaller variance. This method of DOA estimation will be referred to as the Average Histogram (Ave Hist) method.

## 4.2 Average Direction Cosine method

The second method for estimating the DOA for the Phase Gradient and MVDR algorithms was to calculate the average direction cosine values to each Cartesian axis over all the frequency bins, and then perform the required arctangent operation. For horizontal bearings considered here, this is just averaging over the frequency bins the  $\sin(\theta)$  and  $\cos(\theta)$  values of the DOA angle  $\theta$  estimated in each frequency bin. The arctangent is then computed using these averaged values. This procedure will be referred to as the Average Direction Cosine (Ave DC) method.

## 4.3 Simulation results

To estimate the statistics of the different DOA algorithms we performed 100 simulations on each algorithm, each with different seed values for the Gaussian sequence generators, for every SNR value in the range from -9 dB to +12 dB in 3 dB steps. Fig. 7 shows the resulting DOA estimates from all the algorithms for 100 simulations, with SNR -3 dB and the true DOA at  $45^\circ$ . Fig. 8 shows the estimated DOA mean values and corresponding error bars of  $\pm 1$  standard deviation, for all algorithms, as a function of SNR.

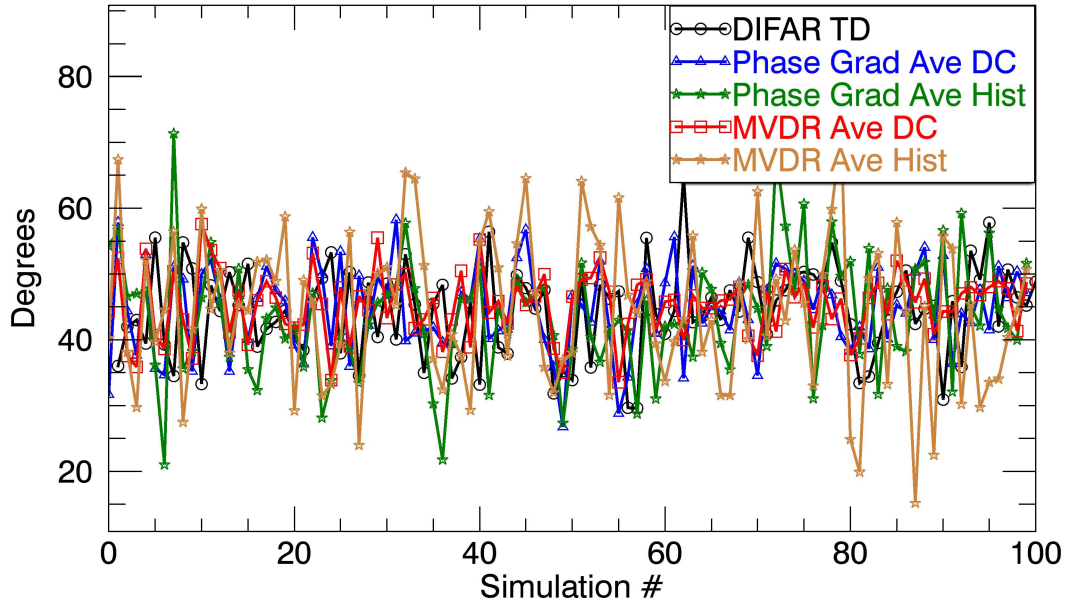


**Figure 7:** Estimates of the DOA from all algorithms for 100 simulations, with SNR -3 dB and the true DOA at  $45^\circ$ .

We can see from Fig. 8 that apart from the MVDR Ave Hist algorithm, the rest of the DOA algorithms give similar results for SNR values above 0 dB. Above 12 dB SNR

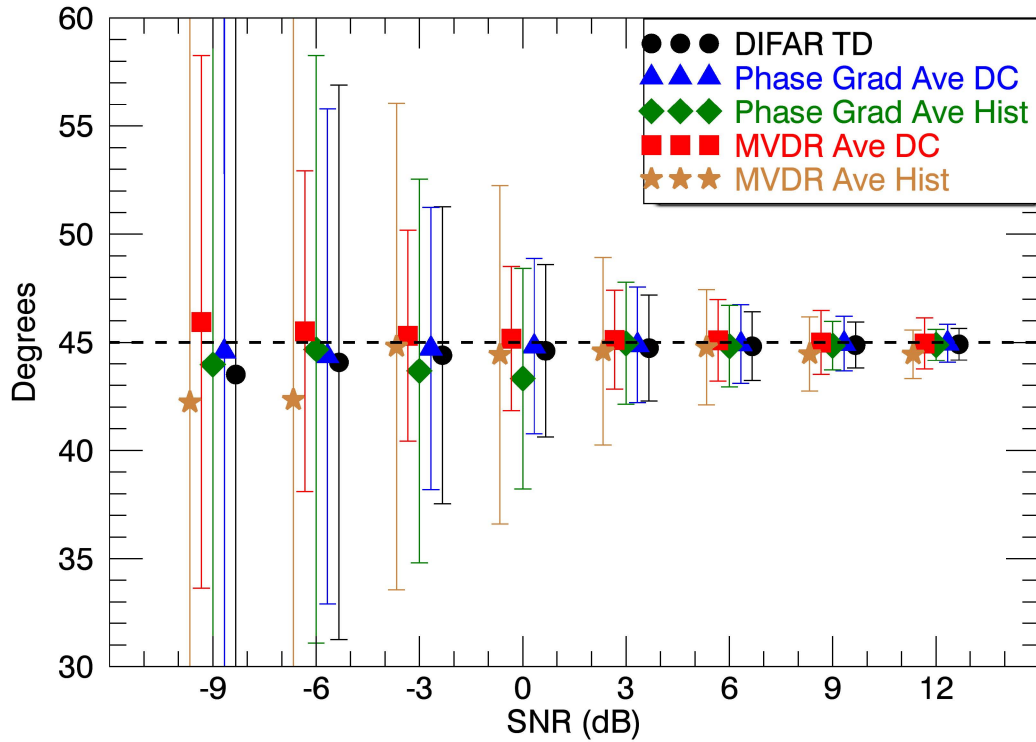


**Figure 8:** Mean and Standard Deviations of the estimated DOA for 100 simulations, as a function of Signal to Noise Ratio (SNR). The true DOA is at  $45^\circ$ , indicated by the dashed line.

we have the standard deviation of all the DOA algorithm estimates at or below  $\approx 1^\circ$ . As the SNR value decreases below 0 dB we can see that the standard deviations of the DOA estimates increase rapidly. The Phase Gradient Ave DC algorithm and to a slightly lesser extent the Phase Gradient Ave Hist algorithm have similar performance to the time-domain DIFAR TD method, showing similar means and standard deviations over the whole range of SNR values. For SNR values below 0 dB the MVDR Ave DC algorithm consistently has the smaller standard deviation of all the algorithms.

## 5 Phase Gradient Histogram Tracking example

Figs. 9 and 10 show the results of the Phase Gradient processing and Histogram Tracking using data collected from a Tetra array. The data was supplied by the German Federal Defence Organization Bundeswehr, under the Next Generation Autonomous Systems (NGAS) NATO Joint Research Project (JRP) agreement. The data was collected at the NGAS 2012 engineering trial in Horten, Norway. The data

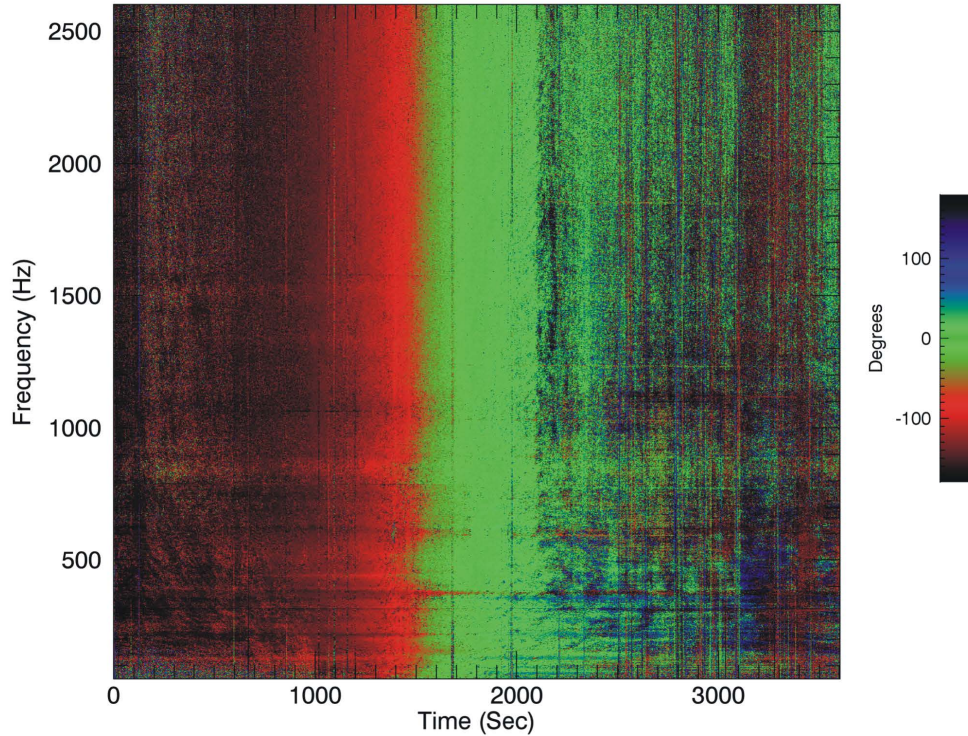


**Figure 9:** Horizontal bearings from the Phase Gradient algorithm, with color coded bearing as a function of time and frequency.

set contains a broad-band acoustic target pass. For this data set the hydrophone sample rate is 20000 Hz. Data was processed from 50 Hz to 2600 Hz using 10000-point FFTs. The frequency band upper limit of the processing is determined by the Tetra array size. The Phase Gradient algorithm requires the maximum array element separation to be less than half a wavelength. The horizontal bearing range was divided into 360 bearing bins, each  $1^\circ$  wide. A total of 15 FFTs were used for the spectral averaging with no overlap, resulting in 480 time windows each 7.5 seconds long. In Fig. 9 we see the Phase Gradient results as color coded horizontal bearing as a function of time and frequency. Fig. 10 shows the Histogram Tracking results, with color coded histogram counts. The broad-band target track for this data set is well defined using the Phase Gradient algorithm and Histogram Tracking procedure, and either the Average Direction Cosine or Average Histogram method gives a good single value estimate for the DOA. Determining when to run the DOA estimate algorithms could be signalled from the Sentinel algorithms once a target is detected, or a threshold level on the histogram count could also be used.



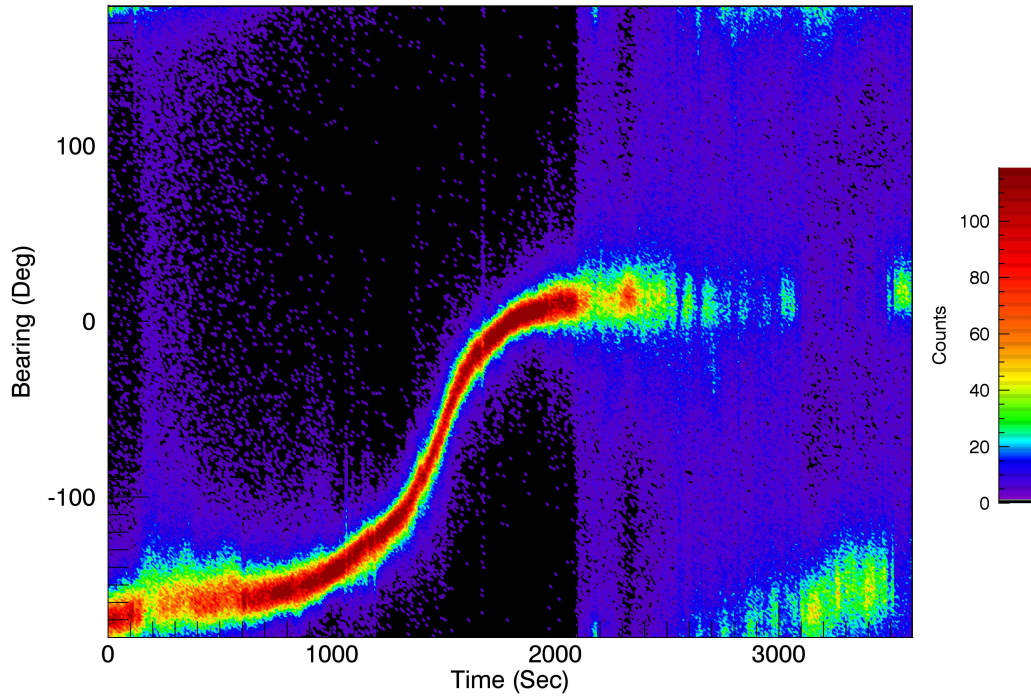


**Figure 10:** Histogram tracking of the horizontal bearing using the Phase Gradient algorithm, with color coded histogram counts.

## 6 Conclusion

On the DRDC Starfish sensor nodes we have time-domain and frequency-domain Sentinel algorithms for target detection implemented. The frequency-domain Acoustic Sentinel algorithm was designed to detect broad-band acoustic targets. The time-domain Acoustic Sentinel algorithm integrates all energy in the band of interest and does not depend on the spectral shape of the signal. Since both can be running simultaneously, differences in their detections could be used to flag different target types or unusual acoustic environments.

The Phase Gradient algorithm performance in determining the DOA of a broad-band signal was evaluated using computer simulations and tested experimentally. Two methods were examined that combined the bearing information from each FFT frequency bin into one DOA estimate; the Average Direction Cosine (Ave DC) and the Average Histogram (Ave Hist) methods. Results from the Phase Gradient algorithm were compared to those from the MVDR and the standard time-domain DIFAR TD DOA algorithms. The Phase Gradient algorithm using the Ave DC method gave similar DOA estimates with similar standard deviations as the DIFAR TD algorithm over all SNR values. The Phase Gradient Ave Hist algorithm gave slightly larger standard

deviations below 0 dB than the DIFAR TD. Above 0 dB SNR all the algorithms performed well. Below 0 dB SNR the standard deviations of the DOA estimates increased, with the MVDR Ave DC algorithm having the smallest standard deviation, while the other algorithms performed similarly, except for the MVDR Ave Hist algorithm which had a consistently larger standard deviation for reasons unknown.

For detecting a broad-band DOA signal the DIFAR TD, Phase Gradient Ave DC, and MVDR Ave DC algorithms all performed similarly above 0 dB, with the MVDR Ave DC algorithm having smaller standard deviations below 0 dB. For an embedded system with limited processing power the Phase Gradient Ave DC and DIFAR TD algorithms would have the advantage over the MVDR algorithm because they require much less processing power. Since the Phase Gradient algorithm is applied in the frequency domain, it would have the advantage if processing of particular frequency bands was required. One such example might be the tracking of a target using its tonal lines and associated harmonics.

The Phase Gradient algorithm has the disadvantage of only being applicable to very symmetric array shapes, such as the crossed-dipole or tetrahedral arrays. The MVDR algorithm can be applied to a general array shape, and also has the advantage of being able to resolve the DOA of more than one arrival simultaneously. The Phase Gradient algorithm is much more efficient than the MVDR algorithm and is more applicable to embedded systems with limited processing power. In a tracking system the Phase Gradient algorithm would be simple to implement because it automatically gives the bearing without searches. The MVDR algorithm may require a complex tracking algorithm to follow the target from update to update to reduce processing requirements by only searching over look directions near the DOA from the previous update.

The frequency-domain and histogram tracking results presented in Figs. 9 and 10 from the Phase Gradient algorithm give an experienced observer a great deal of information about the frequency content and tracking effectiveness for a target. These would be useful real-time displays when tracking a target from a shore station where the underwater sensors would be cabled to shore. Because of the efficiency of the Phase Gradient algorithm it may be more possible to create real-time updated displays such as these on typical computers than with the MVDR algorithm.

This page intentionally left blank.



# References

---

- [1] Otnes, R. (May 2012), NILUS - An Underwater Acoustic Network Demonstration System, *10th International Mine Warfare Technology Symposium*. Monterey, California, USA.
- [2] Lucas, C., Heard, G., and Pelavas, N. (2013), The Phase Gradient Bearing Estimation Algorithm, *Proceedings of Meetings on Acoustics (POMA)*.
- [3] Datta, U., Otnes, R., and Lucas, C. (Sep. 2010), Bearing estimation using small tetrahedral passive hydrophone array, *Oceans Conference*. Seattle Wash.
- [4] Davies, S. (Sep. 1987), Bearing accuracies for arctan processing of crossed dipole arrays, *Oceans Conference*. Halifax, NS.
- [5] Maranda, B. (Sep. 2003), The statistical accuracy of an arctangent estimator, *Oceans Conference*. Pages(s) 2127-2132 Vol.4.

This page intentionally left blank.

DOCUMENT CONTROL DATA		
(Security markings for the title, abstract and indexing annotation must be entered when the document is Classified or Designated.)		
1. ORIGINATOR (The name and address of the organization preparing the document. Organizations for whom the document was prepared, e.g. Centre sponsoring a contractor's report, or tasking agency, are entered in section 8.)  <b>DRDC – Atlantic Research Centre</b> <b>PO Box 1012, Dartmouth NS B2Y 3Z7, Canada</b>		2a. SECURITY MARKING (Overall security marking of the document, including supplemental markings if applicable.)  <b>UNCLASSIFIED</b>
		2b. CONTROLLED GOODS  <b>(NON-CONTROLLED GOODS)</b> <b>DMC A</b> <b>REVIEW: GCEC APRIL 2011</b>
3. TITLE (The complete document title as indicated on the title page. Its classification should be indicated by the appropriate abbreviation (S, C or U) in parentheses after the title.)  <b>DRDC Starfish Acoustic Sentinel and Phase Gradient Histogram Tracking</b>		
4. AUTHORS (Last name, followed by initials – ranks, titles, etc. not to be used.)  <b>Lucas, C. E.; Heard, G. J.; Pelavas, N.</b>		
5. DATE OF PUBLICATION (Month and year of publication of document.)  <b>April 2015</b>	6a. NO. OF PAGES (Total containing information. Include Annexes, Appendices, etc.)  <b>26</b>	6b. NO. OF REFS (Total cited in document.)  <b>5</b>
7. DESCRIPTIVE NOTES (The category of the document, e.g. technical report, technical note or memorandum. If appropriate, enter the type of report, e.g. interim, progress, summary, annual or final. Give the inclusive dates when a specific reporting period is covered.)  <b>Scientific Report</b>		
8. SPONSORING ACTIVITY (The name of the department project office or laboratory sponsoring the research and development – include address.)  <b>DRDC – Atlantic Research Centre</b> <b>PO Box 1012, Dartmouth NS B2Y 3Z7, Canada</b>		
9a. PROJECT OR GRANT NO. (If appropriate, the applicable research and development project or grant number under which the document was written. Please specify whether project or grant.)  <b>01CL01</b>	9b. CONTRACT NO. (If appropriate, the applicable number under which the document was written.)	
10a. ORIGINATOR'S DOCUMENT NUMBER (The official document number by which the document is identified by the originating activity. This number must be unique to this document.)  <b>DRDC-RDDC-2015-R025</b>	10b. OTHER DOCUMENT NO(s). (Any other numbers which may be assigned this document either by the originator or by the sponsor.)	
11. DOCUMENT AVAILABILITY (Any limitations on further dissemination of the document, other than those imposed by security classification.) <input checked="" type="checkbox"/> (X) Unlimited distribution <input type="checkbox"/> ( ) Defence departments and defence contractors; further distribution only as approved <input type="checkbox"/> ( ) Defence departments and Canadian defence contractors; further distribution only as approved <input type="checkbox"/> ( ) Government departments and agencies; further distribution only as approved <input type="checkbox"/> ( ) Defence departments; further distribution only as approved <input type="checkbox"/> ( ) Other (please specify):		
12. DOCUMENT ANNOUNCEMENT (Any limitation to the bibliographic announcement of this document. This will normally correspond to the Document Availability (11). However, where further distribution (beyond the audience specified in (11)) is possible, a wider announcement audience may be selected.)		

13. ABSTRACT (A brief and factual summary of the document. It may also appear elsewhere in the body of the document itself. It is highly desirable that the abstract of classified documents be unclassified. Each paragraph of the abstract shall begin with an indication of the security classification of the information in the paragraph (unless the document itself is unclassified) represented as (S), (C), or (U). It is not necessary to include here abstracts in both official languages unless the text is bilingual.)

DRDC - Atlantic Research Centre, an agency of the Canadian Department of National Defence, has developed a prototype multi-influence underwater surveillance sensor called the Starfish. The Starfish has acoustic, electric, and magnetic field sensors, and onboard signal processing for target detection and tracking. The acoustic sensors are in the form of a seven-element cross-dipole hydrophone array, with two hydrophones along each orthogonal axis direction and one at the array centre.

Acoustic target detection is performed using both time-domain and frequency-domain Sentinel algorithms. The Sentinel algorithms use parallel exponential filters, with the frequency-domain algorithm using parallel filters in each frequency bin.

A Phase Gradient bearing estimation algorithm is used to perform the acoustic target tracking. This is a frequency-domain algorithm that estimates the gradient of the spatial phase of the incoming acoustic signal, and directly computes the wavevector of the acoustic arrival in each frequency bin. A Histogram Tracking procedure is used to display and determine the track angles for a broad-band acoustic target. This paper will discuss the details of the frequency-domain Acoustic Sentinel algorithm and the Phase Gradient bearing estimation algorithm with Histogram Tracking.

14. KEYWORDS, DESCRIPTORS or IDENTIFIERS (Technically meaningful terms or short phrases that characterize a document and could be helpful in cataloguing the document. They should be selected so that no security classification is required. Identifiers, such as equipment model designation, trade name, military project code name, geographic location may also be included. If possible keywords should be selected from a published thesaurus. e.g. Thesaurus of Engineering and Scientific Terms (TEST) and that thesaurus identified. If it is not possible to select indexing terms which are Unclassified, the classification of each should be indicated as with the title.)

DRDC Scientific Report; hydrophone, detection, bearing, histogram



# DRDC | RDDC

**SCIENCE, TECHNOLOGY AND KNOWLEDGE**  
FOR CANADA'S DEFENCE AND SECURITY

**SCIENCE, TECHNOLOGIE ET SAVOIR**  
POUR LA DÉFENSE ET LA SÉCURITÉ DU CANADA



[www.drdc-rddc.gc.ca](http://www.drdc-rddc.gc.ca)